Ultrastructure of the Contractile Apparatus of Rat Skeletal Muscle Embedded in an Aqueous Medium

A. JAKUBIEC-PUKA[1,3], D. FRÖSCH[2] and R. RÜDEL[1]

1 *Abteilung für Allgemeine Physiologie der Universität Ulm, D-7900 Ulm, Federal Republic of Germany*
2 *Sektion Elektronenmikroskopie der Universität Ulm, Oberer Eselsberg, D-7900 Ulm, Albert Einstein-Allé 11, Federal Republic of Germany*
3 *Laboratory of Protein Metabolism, Nencki Institute of Experimental Biology, 3 Pasteur Street, PL-02-093 Warsaw, Poland*

Abstract. The method of tissue embedding in melamine resin was applied to rat skeletal muscle. This method does not require tissue dehydration with organic solvents; only aqueous solutions are used. Electron micrographs of muscles embedded in melamine differ from those embedded in the conventional epoxy resin. In melamine-embedded muscles the actin and myosin filaments appear larger in diameter and subunits can be recognized in cross-sectioned myosin filaments. Within the Z-line, the characteristic patterns described for muscles embedded in epoxy resin are not visible; the spaces between the actin filaments are filled with electron-dense material. This suggests that the Z-line is more compact than could be concluded from epoxy resin-embedded muscle specimens. The M-line appears to be different from what is observed in epoxy-embedded muscle. The membranes appear as several clearly delineated layers. Dehydration rather than the action of the organic solvents per se is the main reason for the differences in the structure of the contractile apparatus between melamine- and epoxy-embedded muscles.

Key words: Electron microscopy — Embedding — Dehydration — Skeletal muscle — Filament dimensions — Z-line

Introduction

Electron microscopic studies of thin sections of muscle tissue embedded in a non-polar epoxy resin (Epon) had considerable influence on our knowledge about the ultrastructure of the contractile apparatus in striated muscle. The embedding technique with epoxy resin requires dehydration of the specimen with organic solvents, a procedure likely to have untoward effects on tissue

Reprint requests to Dr. Rüdel

ultrastructure (Maupin-Szamir and Pollard 1978; Small 1981; Baschong et al. 1984). Recently a novel resin for tissue embedding has been introduced, which does not require the dehydration step (Bachhuber and Frösch 1983). The melamine resin (Nanoplast^R) is water-soluble; therefore, organic solvents are unnecessary. We embedded mammalian muscle in melamine resin and report here ultrastructural details seen in electron micrographs from ultrathin sections of such muscles. In particular, differences to the ultrastructure as observed in muscles embedded in the conventional epoxy resin have been stressed. Preliminary accounts of this work appeared elsewhere (Jakubiec-Puka and Frösch 1985; Jakubiec-Puka et al. 1986).

Materials and Methods

Whole leg muscles (soleus, SOL, and extensor digitorum longus, EDL) from 2.5 to 3-months-old female Wistar rats were used. The muscles were set at rest length, fixed and cut in blocks as described elsewhere (Jakubiec-Puka et al. 1981). Specimens were fixed and embedded with a standard method including fixation in a solution containing 2 % glutaraldehyde, 2 % tannic acid (Mallinckrodt, St. Louis, MO, USA), 2 % sucrose and 0.1 mol/l sodium phosphate buffer (pH 7.2), staining en bloc with 1 % aqueous uranyl acetate and embedding in a 50 % aqueous solution of hexamethylol-melamine-ether (Nanoplast, Balzers AG, Balzers, Liechtenstein) according to Bachhuber and Frösch (1983). The aldehyde-fixed muscle samples infiltrated by (50 % aqueous) Nanoplast were hardened by a two-step procedure. First, the samples were placed for two days in an oven at 40 °C. During this period, water evaporates and, consequently, the resin solution decreases in volume by about 50 % without being polymerized. Subsequently, the samples were transferred to 60 °C, for polymerization (24 to 48 hours).

To discriminate between the effect of dehydration and a possible intrinsic action of the conventional organic solvents, ethanol and propylene oxide, on the ultrastructural appearance of the muscle tissue the following procedures were run in parallel:

I. Standard fixation and staining with
   (a) standard embedding;
   (b) dehydration in a series of ethanol-water mixtures with decreasing water content, rehydration by application of the same solution series in the opposite sequence, followed by standard embedding;
   (c) dehydration as in (b) plus application of propylene oxide, rehydration as in (b), and standard embedding;
   (d) dehydration as in (c), rehydration by immediate transition to 100 % water, standard embedding; and
   (e) dehydration as in (c) followed by embedding in epoxy resin.

II. Standard fixation without staining; standard embedding.

III. Fixation in 2.5 % glutaraldehyde and 2 % paraform-aldehyde (the modified method of Karnovsky 1965) followed by
   (a) standard embedding; or
   (b) standard staining en bloc with 1 % aqueous uranyl acetate and standard embedding;
   (c) postfixation in 1 % osmium tetroxide and standard embedding;
   (d) postfixation in 1 % osmium tetroxide, dehydration and embedding in epoxy resin as in Ie.

To test the influence of the ionic strength of the postfixation medium on the ultrastructural dimensions the specimens were occasionally placed in 0.9 % NaCl or 0.5 mol/l sodium acetate instead of water. Also, the embedding procedure was varied by keeping specimens in 25 % melamine for 24 hours before applying the normal 50 % melamine solution for another 24 hours. All these variations of the standard embedding method had no detectable effects on the ultrastructural details (including the size of the filaments).

Ultrathin sections were made on a Reichert OmU3 microtome or an LKB Ultratome III, using a diamond knife at a speed of 2—5 mm/s. Silver or gray-colored sections (thickness about 50 nm or less) were selected, stained with an aqueous solution of 1 % uranyl acetate and 0.3 % lead citrate. Some sections were studied without any staining. The sections were inspected with a Philips EM 301, a JEM 100B or a Zeiss EM 10A electron microscope. For measurements of ultrastructural dimensions a recently calibrated microscope was used. The microscope was calibrated using calibration specimens of Agar Scientific (Cambridge, UK) containing 6160 lines/mm, ruled at 90° to one another, and with negatively stained catalase crystals. The micrographs of the calibration specimens were taken in parallel with those of the muscle tissue. For the measurement of ultrastructural dimensions, EM photographs were taken at magnification × 45,000 — × 100,000 from sections collected on formvar films. The negatives were projected onto a screen with an additional magnification of × 6.5 or × 17.5, and the dimensions were measured with a ruler. Filaments were measured on cross-sections of the muscle fibres. The diameter of each filament was measured in two or three different planes of the filament profile. The mean value of these measurements was taken as the diameter of the filament. The results were expressed as mean ± SEM of measurements of at least 20 filaments. The results presented in the tables were obtained from series of micrographs measured under the same conditions. To evaluate possible shrinkage of the material during the procedure, the distance between tetragonally arranged actin filaments was measured within the Z-line face region. Only slides showing a distance of about 24 nm between the actin filaments were taken for the study of structure dimensions.

Results and Discussion

Several ultrastructural details seemed much better resolved in electron micrographs made with melamine-embedded muscle than in those with epoxy-embedded muscle. Many new details appeared and several structural dimensions were different (Figs. 1—6, Table 1). The cytoplasmic ground (Wolosewick and Porter 1979; Bridgman 1987) seemed to be recognizable.

Contractile apparatus

Actin filaments. In longitudinal sections of melamine-embedded muscle (Fig. 2) the actin filaments look thicker than in epoxy-embedded muscle. The long-pitch helix geometry of individual actin filaments is visible with "cross over" at about 36 nm, and individual actin molecules seem to be recognizable.

The diameter of the actin filament in transverse section was about 9.5 nm, both in stained (procedures I and III of Methods) and unstained (procedure II)

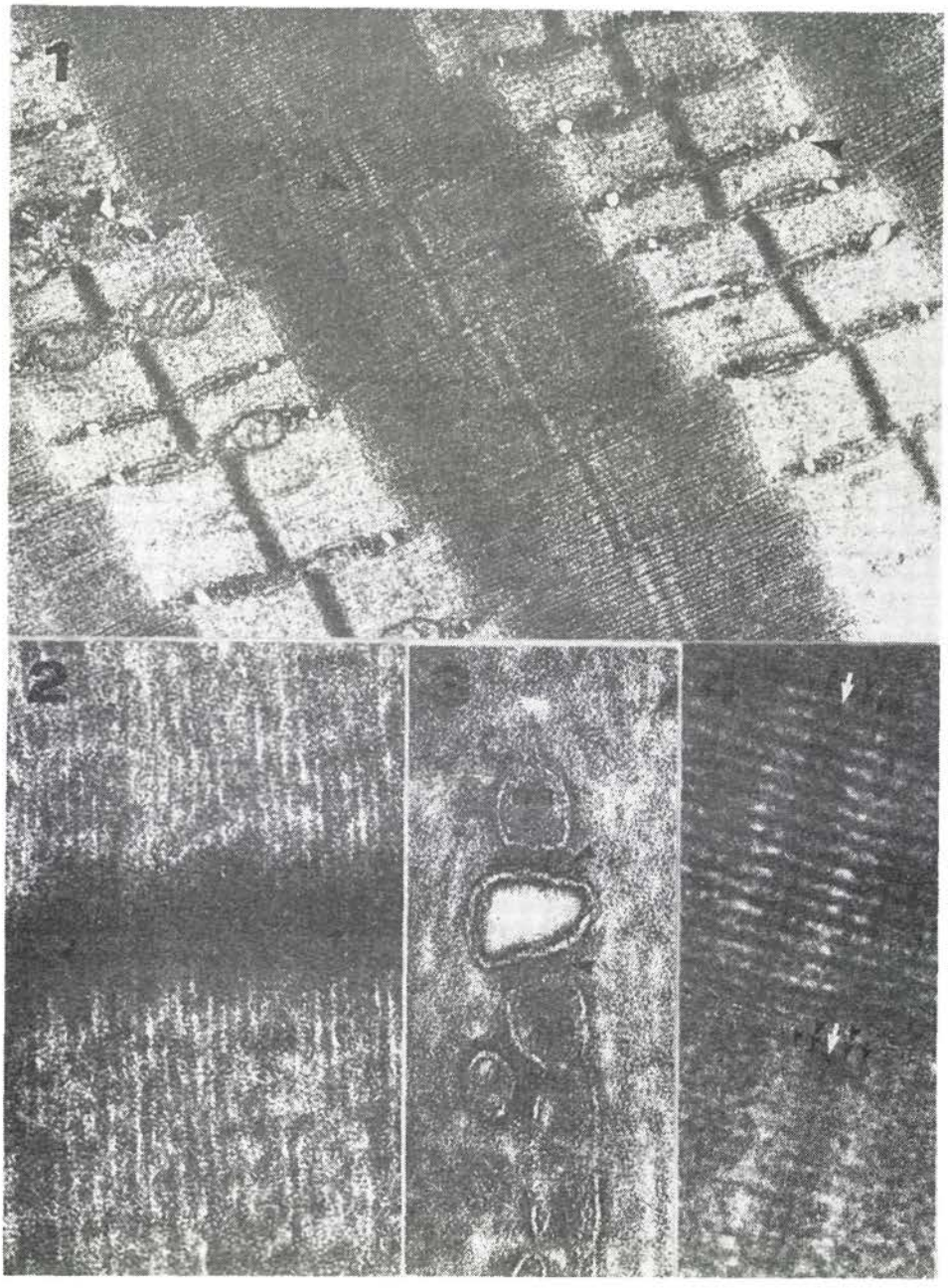

Fig. 1. Melamine-embedded (standard procedure) EDL muscle; longitudinal section. A-band, I-band, Z-line, M-line are well defined. Membranes are clearly outlined. Regions marked by arrows are shown in Figs. 3 and 4. × 31,000

specimens regardless of whether it was determined in the A-band, the I-band or in the face of the Z-line (see Table 1). Dehydration and rehydration of the samples before embedding (procedures Ib-d) had no effect on this value (Table 2).

When tannic acid was used for fixation, the surface of the actin filaments appeared more electron-dense than the central region, giving the impression of an empty core (Fig. 5). The possible reason for this phenomenom is discussed later. "Empty cores" were also seen in actin filaments within the Z-line (Figs. 6, 7). The "core" diameter of melamine-embedded actin filaments was determined as 3.9 ± 0.25, 4.2 ± 0.14, 4.6 ± 0.16 and 4.2 ± 0.14 nm for the A-band, I-band, Z-line face and Z-line proper, respectively.

The diameter of the actin filaments in epoxy-embedded muscle (procedures Ie and IIId) was within the range of 6—8 nm (Table 2), i.e. the same as generally measured with epoxy-embedded muscle. In the last few years however, evidence has accumulated suggesting that the diameter of the actin filament is larger. Egelman and DeRosier (1983) and Egelman and Padron (1984) concluded from images of micrographs and X-ray diffraction patterns of living muscle that the diameter of the actin filament is about 9.5 nm. Taylor and Amos (1983) reported diameters of 9.5 nm from the reconstructed image of S-1-decorated actin filaments. Heuser (1983) observed diameters of 9—11 nm in freeze-dried rotatory-replicated actin filaments. Trinick and coworkers (1985) found diameters of approx. 10 nm in isolated actin filaments embedded in a vitreous medium layer. The same range of diameters was measured in the present work with sarcomeric actin filaments embedded without dehydratation (Table 1 and 2). Thus, the true size of the diameter of the actin filaments in living muscle seems to be 9—10 nm.

Our results thus strongly support the model of the actin filament in which the long axis of each actin subunit projects from the filament axis approximately at right angles (Egelman et al. 1982, 1983; O'Brien et al. 1983; Taylor and Amos 1983). This model generates a filament diameter of at least 9 nm. On the other

Fig. 2. The I-band of melamine-embedded (standard procedure) SOL muscle; longitudinal section. Actin filaments look thicker than those known from epoxy-embedded muscle. Continuation of actin filaments within the Z-line is distinguishable (arrows) in spite of the electron-dense material filling the Z-line. × 153,000

Fig. 3. Triad, part of Fig. 1. Several membrane layers can be distinguished: an electron-transparent layer between electron-dense ones; outside the sarcoplasmic reticulum (SR) vesicles an additional electron-dense layer appears. "Feet" (Franzini-Armstrong 1970) are recognizable (arrows). × 203,000

Fig. 4. The M-line, part of Fig. 1. The M1-bridge (white arrow) is more distinct than M4- and M4'-bridges (double arrows). The M6- and M6'-bridges (black arrows) look like thickenings of myosin filaments. × 112,000

Table 1. Diameter of actin and myosin filaments in melamine-embedded muscle. Samples from SOL and EDL muscles were prepared. For the fixation and staining procedures see Methods. Transverse sections collected on formvar film were taken for measurements. Values are means ± SEM of at least 40 or 90* measurements on at least 2 different muscles.

Procedure	Actin filaments (nm)			Backbone of myosin filaments (nm)	
	A-band	I-band	Z-line face	A-band	M-line
Ia (standard)	9.6 ± 0.18	9.6 ± 0.18	9.4 ± 0.14	15.4 ± 0.19*	17.2 ± 0.24*
II		9.3 ± 0.28	9.4 ± 0.16		
IIIa		9.1 ± 0.15	9.5 ± 0.15	14.5 ± 0.32	16.7 ± 0.21
IIIb		8.5 ± 0.20	8.6 ± 0.18	15.3 ± 0.21	16.8 ± 0.20
IIIc		9.1 ± 0.16	9.4 ± 0.16	14.7 ± 9.16	18.3 ± 0.19

Table 2. Effect of dehydration on actin and myosin filament diameters. Samples from EDL muscle were prepared according to procedures described in Materials and Methods. Samples Ia-e were from the same experiment; * pooled samples from several experiments. Samples Ib-d were de- and rehydrated. Transverse sections collected on formvar film were taken for measurements. Values are means ± SEM of at least 20 or 90* filaments.

Procedure	Actin filaments (nm)			Backbone of myosin filaments (nm)	
	A-band	I-band	Z-line face	A-band	M-line
Ia (standard)	9.4 ± 0.3	9.5 ± 0.3	9.9 ± 0.4	15.4 ± 0.2*	17.2 ± 0.2*
Ib	10.4 ± 0.5	9.6 ± 0.2	9.7 ± 0.2	16.4 ± 0.4	16.4 ± 0.4
Ic	7.9 ± 0.3	9.9 ± 0.3	8.9 ± 0.2	14.5 ± 0.4	17.3 ± 0.4
Id	8.6 ± 0.3	8.9 ± 0.4	9.6 ± 0.6	16.8 ± 0.4	18.3 ± 0.5
Ie	6.9 ± 0.2	7.5 ± 0.3	6.7 ± 0.3	12.0 ± 0.3	12.7 ± 0.2
IIId	6.8 ± 0.2	7.3 ± 0.4	7.4 ± 0.2	12.9 ± 0.4	14.5 ± 0.4

hand, our results do not favour the model of actin filament in which actin monomers are arranged with their long axis parallel to the filament axis (Moore et al. 1970; Suck et al. 1981; Smith et al. 1983; Toyoshima and Wakabayashi 1985). The latter model requires diameters below 8 nm (Suck et al. 1981; Fowler and Aebi 1983).

Z-line. Within the Z-line, the actin filaments showed a simple square arrangement (Fig. 6*A*) with a periodicity corresponding to that of the lattices described for epoxy-embedded muscle (Fig. 6*B*). The interfilament spaces were evenly filled with electron-dense material suggesting that the Z-line is a compact structure (Figs. 2, 6*A*, 7*A*). The typical density distribution of material as "large-square lattice", "small-square lattice" and "basket weave" patterns (for details see Schmalbruch 1985) of epoxy-embedded muscle (Fig. 6*B*) was never

observed in melamine-embedded muscle, irrespective of the procedure preceding embedding (I, II or III), i.e. whether tannic acid or osmium tetroxide was used for fixation and whether the samples were stained en block with uranyl acetate or not. In epoxy-embedded (i.e. dehydrated) muscles the mentioned characteristic patterns were always present, irrespective of the pre-embedding procedures (Ie or IIId, see Figs. 6*B*, 7*C*). The structure and dimensions of the Z-line were very similar in all melamine-embedded muscles, no matter whether organic solvents had been used before embedding or not (Figs. 7*A*, *B*). These observations suggest that the differences in Z-lines observed between melamine- and epoxy-embedded muscle are due to dehydration, rather than to the fixation and/or staining procedures or to the organic solvents per se. Moreover, the reversibility of the dehydration-induced changes make it unlikely that the organic solvents used removed any components such as lipoproteins or hydrophobic proteins.

At the level of the Z-line, membranes were very well recognizable between the myofibrils (Fig. 7*A*), but intermediate filaments (Lazarides et al. 1982) could not be detected.

Myosin filaments. On both longitudinal (Figs. 1, 4) and transverse (Figs. 5, 8*A*, *C*) sections of samples embedded with the melamine standard procedure the myosin filaments were well visible. On transverse sections the outline of the myosin filaments was not always clear and the shape of neighbouring filaments was not uniform. Usually the shape of the filaments showed no well-defined regularity, being in some places circular, in others elliptical or trigonal (also within regions distant from the M-line). This irregularity could be explained by a nonuniform dissociation of the myosin rods from the filament backbones, as described by Trinick and Elliott (1982) and Knight and Trinick (1984).

In melamine embedded muscle the diameter of the transversally sectioned myosin filaments (which seems to represent the filament backbone) was about 15 nm in the A-band and about 17 nm in the M-line, regardless of the procedures of fixation and staining applied (Ia, II, IIIa, c, Tables 1, 2).

In epoxy-embedded muscle the myosin filaments were smaller in diameter, no matter which fixation procedure was applied (Fig. 8, Table 2). The diameters were well in the range of values reported by other authors (Huxley 1971; Squire 1973). In the samples dehydrated and rehydrated before embedding in melamine (procedure Ib-d) the diameter of the myosin filaments was in the range of that seen in samples embedded without previous dehydration (Table 2). This shows that dehydration is the reason for the reduced diameter of myosin filaments in epoxy-embedded muscle, as could be already concluded from the results obtained with actin filaments.

Similar diameters of vertebrate myosin filaments were reported for negatively stained myosin filaments (Knight and Trinick 1984) and calculated on the

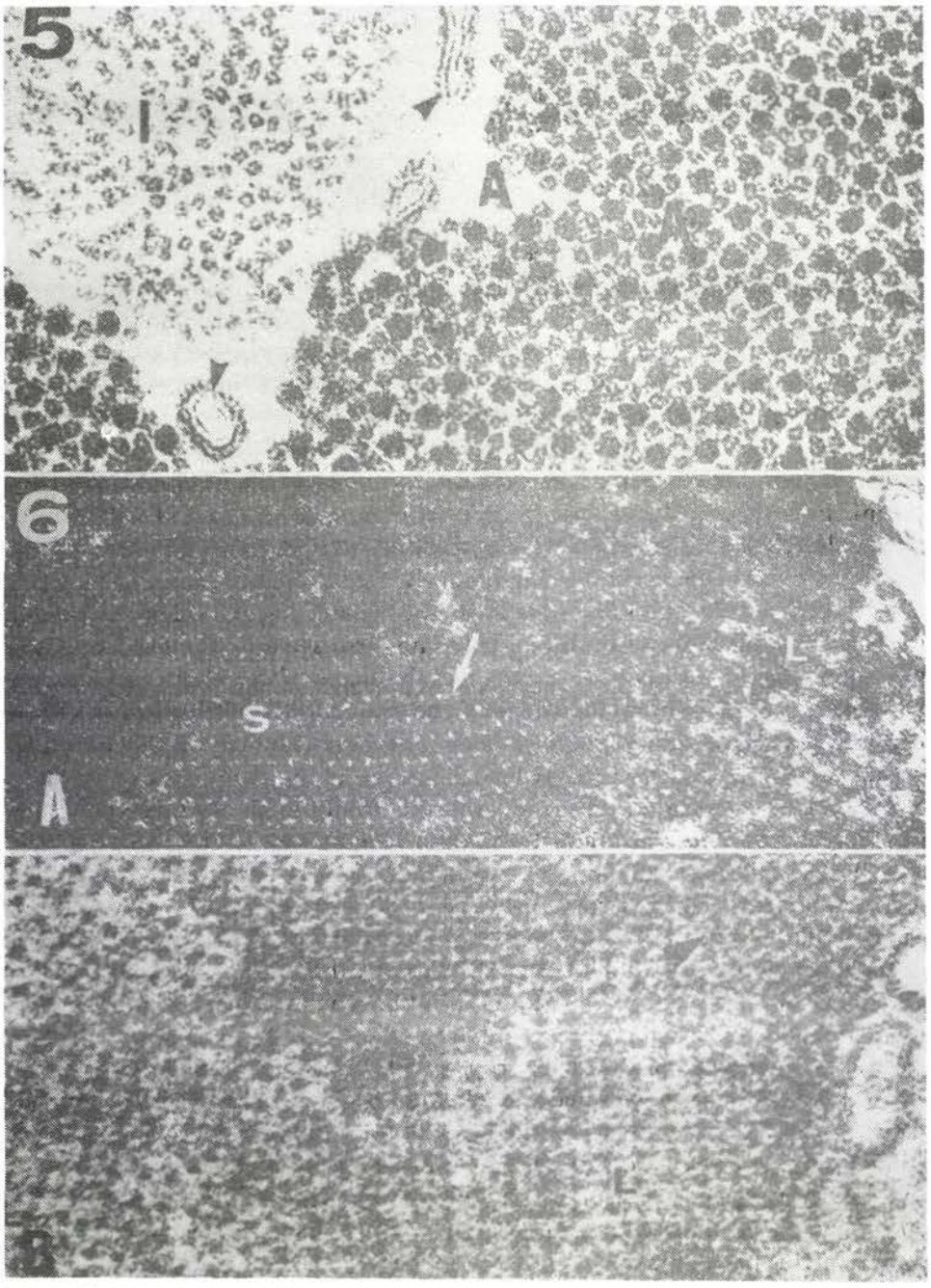

Fig. 5. The A-band (A) and I-band (I) of melamine-embedded (standard procedure) EDL muscle; transverse section. Diameters of both actin and myosin filaments seem to be larger than those known from epoxy-embedded muscle. Actin filaments are stronger contrasted on the surface than in the central region. Subunits are recognizable within myosin filaments. Membranes (arrows) show several layers. × 200,000

basis of Donnan potential measurements (Elliott and Bartels 1982): freeze-dried and shadowed myosin filaments show an even larger diameter (Trinick and Elliott 1982). Thus, similarly as for the actin filaments, melamine embedding seems to give diameter values for myosin filaments that more closely resemble the *in vivo* size.

The cross section of the myosin filament revealed the existence of many subunits (Figs. 5, 8*A*—*D*), minimum 11 and maximum 16 according to our counts. On some tannine-fixed sections these subunits looked as if negatively stained (Figs. 5, 8*C*). This phenomenon is discussed later. The shape and size of the individual subunits were not uniform. Some of them were small and spherical, others were larger and elongated. They differed in number and arrangement. Within individual filaments a symmetry was seen in the distribution of the subunits. Occasionally subunits showed three- or two-fold symmetry; sometimes they resembled rosettes. Optical diffraction analysis (in preparation) will perhaps provide some more information about the size and the organization of the subunits. The myosin filament subunits were also visible after the de- and rehydration cycle (Fig. 8*D*). They could even be recognized on sections embedded in epoxy resin (Figs. 8*E*, *F*).

The number of subunits and their arrangement within the myosin filament appeared to be different from what has been proposed by the models of Squire (1973) and Pepe (1975). More subunits could be seen on our thin sections (about 50 nm) than reported by Pepe (1975, 1982) who investigated sections 3 to 10 times thicker. No regular arrangement of the subunits could be found on our sections, contrary to Pepe who observed 3 centrally and 9 peripherally situated subunits. In addition, our subunits were not uniform either in size or in shape. Neither did we observe real crossbridges corresponding to the symmetrical arrows projecting from the filament surface in Pepe's model. Hence, we believe that the arrangement of the myosin filament subunits within a slice about 50 nm thick is different from that proposed by Pepe on the basis of rather thick sections. Neither do our observations confirm Squire's (1973) ideas concerning the myosin filament. We counted only about half the number of subunits proposed in his model. The diameter of myosin filaments in melamine-embedded muscle, on the other hand, should correspond to Squire's model of the myosin filament.

Fig. 6. The Z-line of SOL muscle; transverse section. *A* — melamine-embedded (standard procedure) and *B* — epoxy-embedded (procedure IIId) muscles. Regions corresponding to "large square lattice" (L), "small square lattice" (S) and "basket weave" (black arrow) patterns are shown. The tetragonal arrangement of the actin filaments is well seen in both muscles. In melamine-embedded muscle electron-dense material fills the spaces between actin filaments in regions corresponding to "small square lattice" and/or "basket weave" patterns. "Empty cores" of actin filaments are seen (white arrow) × 205,000

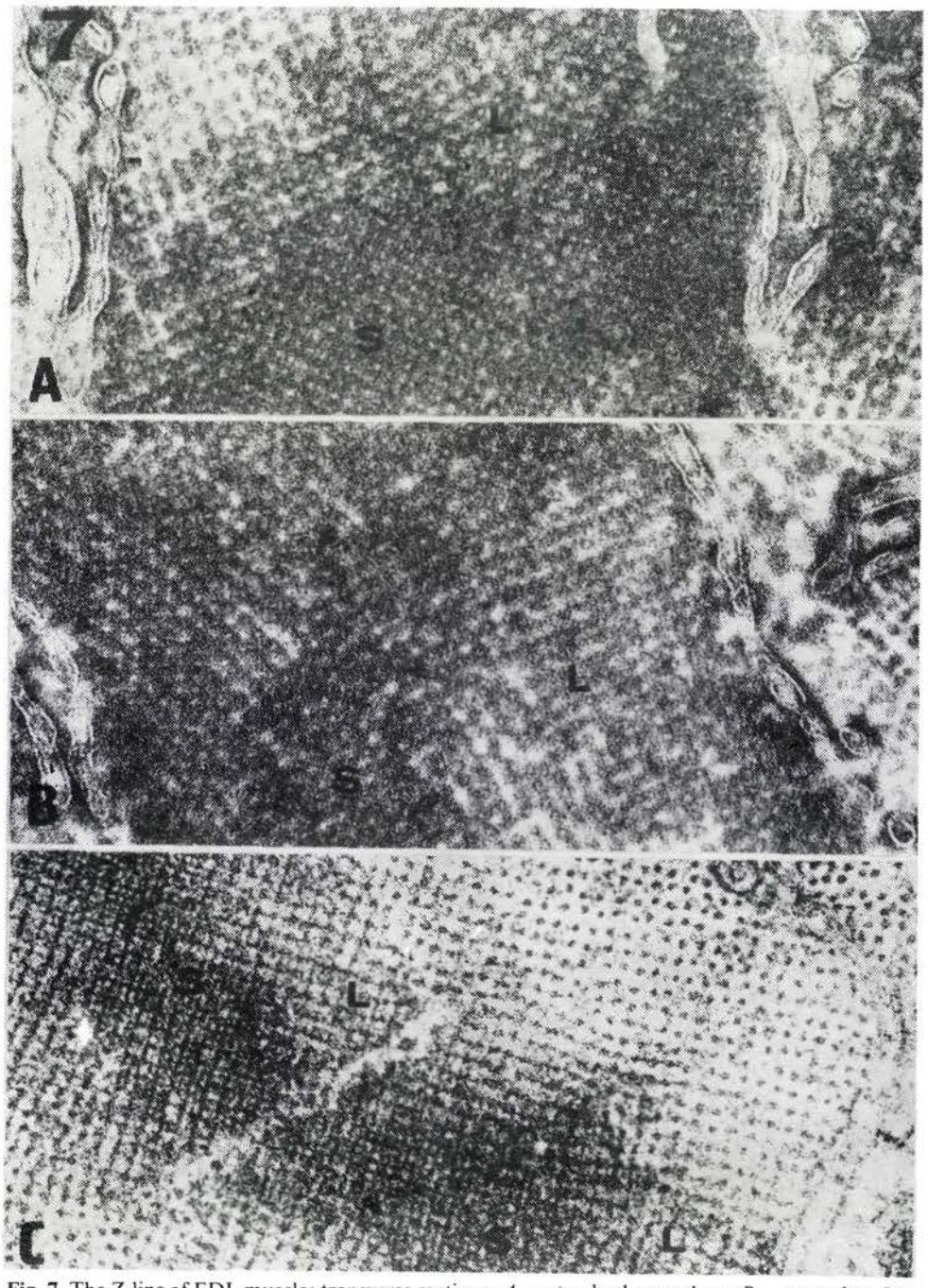

Fig. 7. The Z-line of EDL muscle; transverse sections. *A* — standard procedure; *B* — procedure Ic; *C* — procedure Ie. Regions corresponding to "large-square lattice" (L), "small-square lattice" and/or „basket weave" (S) patterns are seen. Within the Z-line of both melamine-embedded muscles

M-line. Within the M-line of longitudinally sectioned melamine-embedded muscle the known five M-bridges (Sjöström and Squire 1977) could be recognized. The central M1-bridge was usually more distinct than the M4 and M4' bridges, and the M6 and M6' bridges rather resembled thickenings of the myosin filament (Figs. 1, 4). On transverse sections no hollow (Pepe 1975) was seen in the center of the myosin filaments. Only M-bridges (Knappeis and Carlsen 1968; Pepe 1975; Sjöström and Squire 1977) were occasionally visible. The spaces between the myosin filament seemed filled with a fine network (Figs. 9*A*, *B*). Secondary M-bridges (Luther and Squire 1978) or M-filaments (Knappeis and Carlsen 1968), known from the study of epoxy-embedded muscle (Figs. 9*C*, *D*), were observed in melamine-embedded muscle only when the specimens were previously dehydrated. After dehydration and rehydration these structures were sometimes seen (Fig. 9*E*), sometimes not (Fig. 9*B*). We can propose several hypotheses to explain the differences in the M-line between melamine- and expoxy-embedded muscle. The first one assumes that the fine network between myosin filaments within the M-line corresponds to either microtrabeculae (Wolosewick and Porter 1979; Bridgman 1987), or to artificial products of fixation of cytoplasmic proteins. This network, seen better in melamine-embedded samples than in epoxy-embedded ones, makes the M-line elements unrecognizable. The M-line structures themselves become visible when the fine network is destroyed by dehydration. If this is true, the melamine-embedded muscle is not a good object for the study of the M-line ultrastructure. On the other hand, the fine network may represent the M-line structure itself which is destroyed during dehydration and aggregates. In that case, the M-line structures of the epoxy-embedded muscle represent artifacts induced by dehydration. One can imagine that dehydration produces a distortion within the M-line as severe as those observed within the Z-line (Figs. 6, 7) or within actin filaments (Tables 1, 2 and Small 1981). Also, the fine network may represent just cytoplasmic proteins and no other structures than myosin filaments and M-bridges are present within the M-line, as reported for fish muscle (Varriano-Marston et al. 1987). Thus, M-filaments and secondary M-bridges, seen in epoxy-embedded muscle, correspond to the dehydrated lattice of microtrabeculae. These alternatives require a more detailed study.

(*A*, *B*) uncontrasted centers of actin filaments are seen. Electron-dense material appears between tetragonally arranged actin filaments. Membranes are well recognizable between myofibrils. In the dehydrated and rehydrated muscle (*B*) the electron-transparent layer of the membranes seems to be thinner than that in muscle prepared without dehydration (*A*). Within the Z-line of epoxy-embedded muscle (*C*) "large square lattice" and "small-square lattice" are well recognizable. Membranes are poorly outlined as compared with melamine-embedded muscles (*A*, *B*); layers of membranes, however, are still present. *A*, *B*, × 135,000, *C*, × 125,000

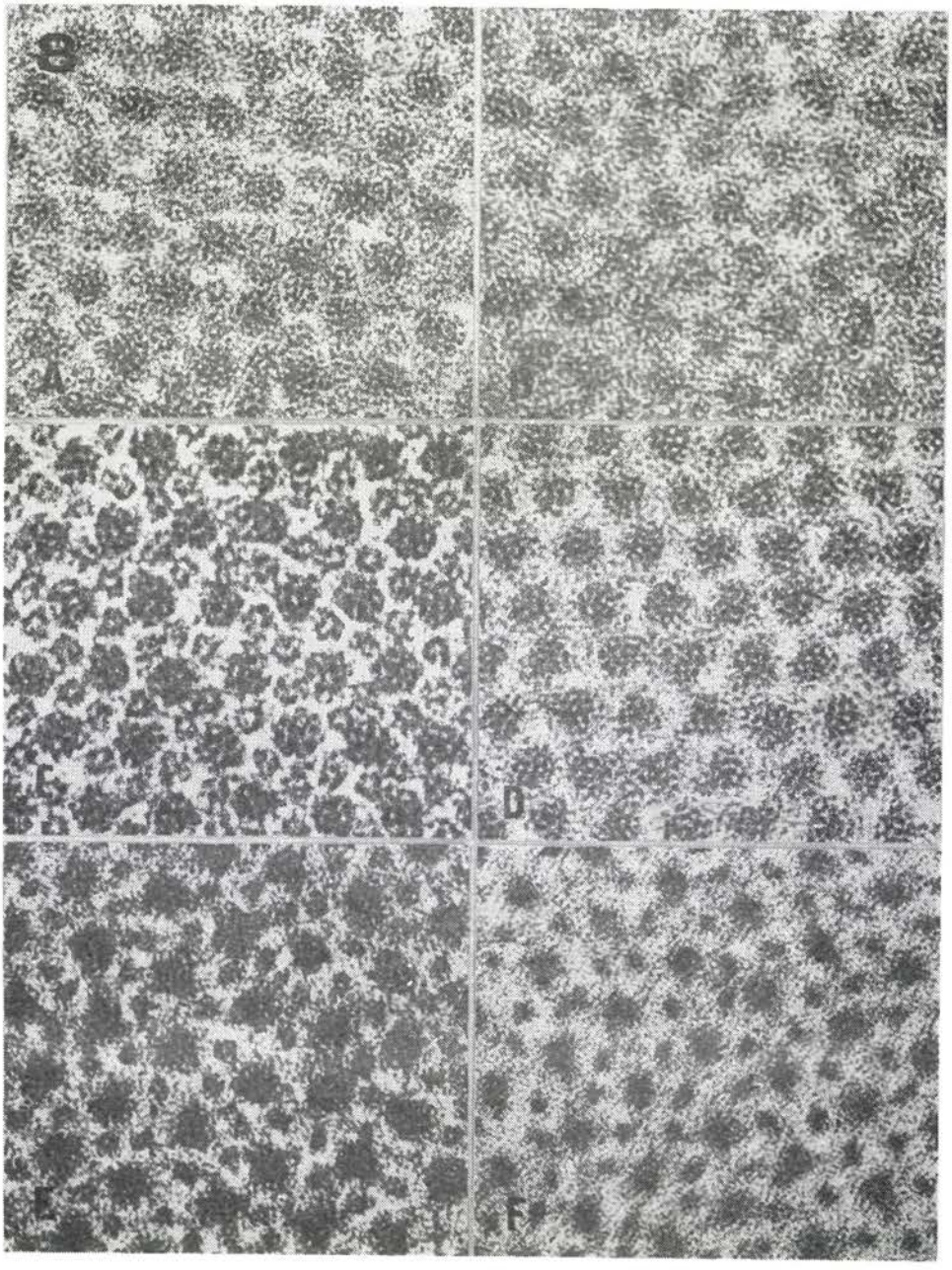

Fig. 8. The A-band; transverse sections. *A* — SOL, standard procedure; *B* — EDL, procedure IIIc; *C* — EDL, standard procedure; *D* — EDL procedure Ic; *E* — EDL. procedure Ie, *F* — EDL, procedure IIId. In melamine-embedded muscles (*A* — *D*) filaments are larger in diameter than in

Membranes

The common picture of a membrane from samples prepared by the standard procedure (Ia) was that of a transparent layer separated by 2 electron-dense layers (Figs. 3, 5, 7*A*). On the outside of SR membranes the electron-dense material was often not clearly delineated and showed a fluffy appearance (Figs. 3, 5). The membrane layers were also observed in dehydrated epoxy-embedded samples when tannic acid was used for fixation (Fig. 7*C*), as reported previously (Kalina and Pease 1977a, b). The electron-dense and -lucent layers correspond to hydrophilic and hydrophobic membrane regions, respectively (Kalina and Pease 1977b). The fluffy appearance outside the SR-membranes (Figs. 3, 5) in melamine-embedded samples corresponds probably to the asymmetry of the SR-membranes observed by Saito et al. (1978) in tannine-fixed, epoxy-embedded samples.

The dehydration/rehydration cycle considerably changed the structural appearance of the membranes: it made layers thinner (compare Figs. 7*A* and *B*) and changed their outlines, so that membranes often appeared wrinkled. The layers, however, were still better preserved than in the dehydrated epoxy-embedded samples (cf. Figs. 7*B* and *C*). The damage to the membranes seems to be the result of both the treatment with organic solvents and the dehydration.

Comments on the methods

Considerable differences in structure and dimension of several organelles were observed between muscles embedded with and without dehydration. The dehydration/rehydration experiments lead us to conclude that dehydration per se is the reason for the bulk of these differences. This is not unexpected considering the degree of protein hydration in the living cell: protein crystals contain 20 % to 90 % water by weight (for a review see Fulton 1982). Thus, a tissue embedded in the hydrated state gives a more natural shape and size of the cell structures, which should be closer to the state *in vivo* than those in dehydrated tissue. In other words, this method of embedding gets rid of dehydration-associated artefacts.

Osmium tetroxide, routinely applied during the preparation of tissues for electron microscopic study, is known to be the reason for considerable artefacts. Osmium tetroxide damages the primary and secondary structure of proteins

epoxy-embedded muscle (*E*, *F*). Subunits are seen within myosin filaments of the melamine-embedded muscles while in epoxy-embedded muscles they are much less recognizable. In tannine-fixed muscles (*A*, *C*, *E*) actin filaments are better contrasted at their surface than the central region. *A*, *B*, *C*, *E*, *F* × 334,000; *D* × 313,000.

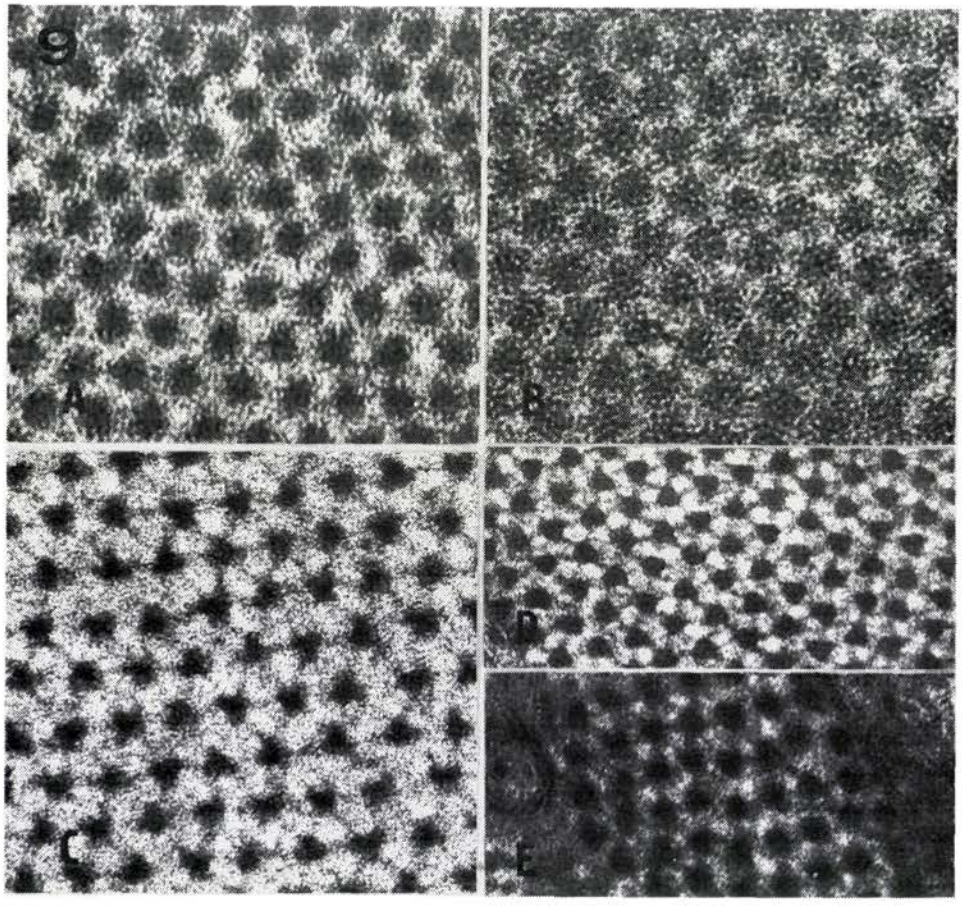

Fig. 9. The M-line of EDL muscle; transverse sections. *A* — standard procedure; *B* — procedure Ic, *C* — procedure IIId; *D* — procedure Ie; *E* — procedure Ib. In melamine-embedded muscle (*A*, *B*) subunits are seen within myosin filaments. The spaces between myosin filaments resemble a network. M-bridges are recognizable in some places. In epoxy-embedded muscles (*C*, *D*) myosin filaments are smaller in diameter than those in melamine-embedded muscle; M-bridges and secondary M-bridges are seen. In dehydrated and rehydrated muscle, structures resembling M-bridges and secondary M-bridges may appear (*E*). *A*, × 222,000; *B*, × 260,000; *C*, × 205,000; *D*, × 157,000; *E*, × 161,000.

making proteins soluble after their initial gelation. Osmium tetroxide distorts cell organelles (Porter and Kallman 1953; Maupin-Szamir and Pollard 1978; Wolosewick and Porter 1979; Baschong et al 1984; Small 1981; Reedy et al 1983). Omission of osmium tetroxide from the standard procedure in this work abolished potent reason of artefacts. Glutaraldehyde is an effective crosslinking reagent for electron microscopy (Sabatini et al. 1963). It only minimally distorts

the structure of proteins; especially when used together with tannic acid (Meek 1981; Baschong et al. 1984) as was the case in the present work. The inaccuracy produced by glutaraldehyde comes from the nonuniform distribution of staining ions rather than from changes in the conformational state of proteins (Meek and Chapman 1985). However, Reedy et al. (1983) observed shrinkage of spacing of the filament lattice in glycerinated insect flight muscle following treatment with 5% glutaraldehyde. This shortcoming can be suspected also in our samples, in spite of the lower concentration of glutaraldehyde used. The possible shrinkage of material can decrease the dimensions of organelles. Thus the true dimensions of structures may be larger than those shown in this work. Both glutaraldehyde and osmium tetroxide can damage actin filaments devoid of tropomyosin (Maupin-Szamir and Pollard 1978; Lehrer 1981). This artefact is rather improbable in actin filaments fixed in the native state, as in this work.

Tannic acid is a very sensitive fixative of proteins, polypeptides and some phospolipids. It acts as multivalent agent and precipitates proteins forming with them insoluble heavy metal chelate compounds. Tannic acid preserves very well cell organelles, such as microtubules, microfilaments or membranes (Mizuhira and Futaesaku 1972; Tilney et al. 1973; Saito et al. 1978; Mizuhira et al. 1981; Kalina and Pease 1977a, b). Osmium tetroxide stabilizes complexes of tannic acid with phosphatides against dissociation with organic solvents (Kalina and Pease 1977a). The omission of organic solvents during fixation allows deletion of osmium tetroxide without loss of clarity of the appearance of membranes.

The reaction of tannic acid with proteins is selective, depending on the pH. At neutral pH, as used in this work, tannic acid precipitates mainly basic proteins, phosphoproteins (Mizuhira and Futaesaku 1972; Mizuhira et al. 1981), Ca-bound proteins (Slocum and Roux 1982) glycoproteins (Chew 1980) and also phosphatides containing choline (Kalina and pease 1977a). Thus structures containing these compounds as well as hydrophilic regions of macromolecules are expected to be especially well preserved and strongly contrasted. This selectivity may be the reason for the "negative staining" effect (Mizuhira and Futaesaku 1972; 1974; Tilney et al. 1973) observed in both melamine- and epoxy-embedded samples (Figs. 8*C*, *E*). Tannic acid has been found to produce a focally higher concentration of calcium and phosphorus (Wacker et al. 1986). When applied *in vivo*, it increases the diameter of microfilaments of radish root (Seagull and Heath 1979). These artefacts produced by tannic acid, if present in our samples, did not influence the dimension of the structures examined, as shown by the similar values obtained with samples fixed with and without tannic acid (Table 1, Fig. 8).

Melamine is very sensitive to the action of electron beams. Under an electron beam melamine sections shrink and split (but are not extended). When

carbon film is used, this disadvantageous phenomenon is abolished or considerably reduced. We tried to diminish the shrinkage by shortening the time of exposure; we cannot, however, exclude some shrinkage in each case, especially when sections were studied without carbon film. The dimensions of structures may, therefore, be de facto larger than presented.

The known phenomenon of stain migration following electron irradiation (Unwin 1974) which can apparently distort the dimensions and the shape of organelles was also taken into consideration. This phenomenon may be neglected in this work because of the short time of exposure to the electron beam.

Acknowledgements. The work was performed while Dr. Jakubiec-Puka was a Visiting Professor at the University of Ulm. The support by the Deutsche Gesellschaft zur Bekämpfung der Muskelkrankheiten is acknowledged.

References

Bachhuber K., Frösch D. (1983): Melamine resins, a new class of watersoluble embedding media for electron microscopy. J. Microsc. **130,** 1—9

Baschong W., Baschong-Prescianotto C., Wurtz M., Carlemalm E., Kellenberger C., Kellenberger E. (1984): Preservation of protein structures for electron microscopy by fixation with aldehydes and/or OsO_4. Eur. J. Cell Biol. **35,** 21—26

Bridgman P. (1987): Structure of cytoplasm as revealed by modern electron microscopy technique. TINS **10,** 321—325

Chew E. C. (1980): On tannic acid fixation and staining. Acta Anat. **108,** 156—159

Egelman E. H., DeRosier D. J. (1983): A model for F-actin derived from image analysis of isolated filaments. J. Mol. Biol. **166,** 623—629

Egelman E. H., Francis N., DeRosier D. J. (1982): F-actin is a helix with a random variable twist. Nature **298,** 131—135

Egelman E. H., Padron R. (1984): X-ray diffraction evidence that actin is a 100 Å filament. Nature **307,** 56—58

Elliott G. F., Bartels E. M. (1982): Donnan potential measurements in extended hexagonal polyelectrolyte gels such as muscle. Biophys. J. **38,** 195—199

Fowler W. E., Aebi U. (1983): A consistent picture of the actin filament related to the orientation of the actin molecule. J. Cell Biol. **97,** 264—269

Franzini-Armstrong C. (1970): Studies of the triad. I. Structure of the junction in frog twitch fibers. J. Cell Biol. **47,** 488—499

Fulton A. B. (1982): How crowded is the cytoplasm? Cell **30,** 345—347

Heuser J. E. (1983): Procedure for freeze-drying molecules adsorbed to mica flakes. J. Mol. Biol. **169,** 155—195

Huxley H. E. (1971): The structural basic of muscular contraction. Proc. Roy. Soc. (London) B **178,** 131—149

Jakubiec-Puka A., Frösch D. (1985): Ultrastructure of aqueous-embedded skeletal muscle. Pflügers Arch. **403,** R58

Jakubiec-Puka A., Frösch D., Rüdel R. (1986): Ultrastructure of the contractile apparatus of muscle embedded in an aqueous medium. J. Muscle Res. Cell Motil. **7,** 77

Jakubiec-Puka A., Kulesza-Lipka D., Krajewski K. (1981): The contractile apparatus of striated muscle in the course of atrophy and regeneration. I. Myosin and actin filaments in the denervated rat soleus. Cell Tissue Res. **220,** 651—663

Kalina M., Pease D. C. (1977a): The preservation of ultrastructure in saturated phosphatidyl cholines by tannic acid in model systems and type II pneumocytes. J. Cell Biol. **74,** 726—741

Kalina M., Pease D. C. (1977b): The probable role of phosphatidylcholines in the tannic acid enhancement of cytomembrane electron contrast. J. Cell Biol. **74,** 742—746

Karnovsky M. J. (1965): A formaldehyde-glutaraldehyde fixative of high osmolality for use in electron microscopy. J. Cell Biol. **27,** 137A—138A

Knappeis G. G., Carlsen F. (1968): The ultrastructure of the M-line in skeletal muscle. J. Cell Biol. **38,** 202—211

Knight P., Trinick J. (1984): Structure of the myosin projections on native thick filaments from vertebrate skeletal muscle. J. Mol. Biol. **177,** 461—482

Lazarides E., Granger B. L., Gard D. L., O'Connor C. M., Breckler J., Price M., Danto S. I. (1982): Desmin- and vimentin-containing filaments and their role in the assembly of the Z disc in muscle cells. Cold Spring Harbor Symposia on Quantitative Biology Vol. XLVI, pp. 351—378

Lehrer S. S. (1981): Damage to actin filaments by glutaraldehyde: protection by tropomyosin. J. Cell Biol. **90,** 459—466

Luther P., Squire J. (1978): Three-dimensional structure of the vertebrate muscle M-region. J. Mol. Biol. **125,** 313—324

Maupin-Szamier P., Pollard T. D. (1978): Actin filament destruction by osmium tetroxide. J. Cell Biol. **77,** 837—852

Meek K. M. (1981): The use of glutaraldehyde and tannic acid to preserve reconstituted collagen for electron microscopy. Histochemistry **73,** 115—120

Meek K. M., Chapman J. A. (1985): Glutaraldehyde-induced changes in the axially projected fine structure of collagen fibrils. J. Mol. Biol. **185,** 359—370

Mizuhira V., Futaesaku Y. (1972): New fixation for biological membranes using tannic acids. Acta Histochem. Cytochem. **5,** 233—235

Mizuhira V., Futaesaku Y. (1974): Fine structure of the microtubules by means of the tannic acid fixation. Proceedings of the Eighth Intern. Congress on Electron Microscopy, Canberra **2,** 340—341

Mizuhira V., Shiihashi K. M., Futaesaku Y. (1981): High-speed electron microscope autoradiographic studies of diffusible compounds. J. Histochem. Cytochem. **29,** 143—160

Moore P. B., Huxley H. E., DeRosier D. J. (1970): Three-dimensional reconstruction of F-actin, thin filaments and decorated thin filaments. J. Mol. Biol. **50,** 279—295

O'Brien E. J., Couch J., Johnson G. R. P., Morris E. P. (1983): Structure of actin and the thin filament. In: Actin, Structure and Function in Muscle and Non-muscle Cells (Eds. dos Remedios, C. G., Barden J. A.), pp. 3—15, Academic Press, Sydney

Pepe F. A. (1975): Structure of muscle filaments from immunohistochemical and ultrastructural studies. J. Histochem. Cytochem. **23,** 543—562

Pepe F. A. (1982): The structure of vertebrate skeletal-muscle myosin filaments. In: Cell and Muscle Motility (Eds. Dowben R. M., Shay J. W.), Vol. 2, pp. 141—171, Plenum, New York

Porter K. R., Kallman F. (1953): The properties and effects of osmium tetroxide as a tissue fixative, with special reference to its use for electron microscopy. Exp. Cell Res. **4,** 127—141

Reedy M. K., Goody R. S., Hofmann W., Rosenbaum G. (1983): Co-ordinated electron microscopy and X-ray studies of glycerinated insect flight muscle. I. X-ray diffraction monitoring during preparation for electron microscopy of muscle fibres fixed in rigor, in ATP and AMPPNP. J. Muscle Res. Cell Motil. **4,** 25—53

Sabatini D. D., Bensch K., Barrnett R. J. (1963): Cytochemistry and electron microscopy. The

preservation of cellular ultrastructure and enzymatic activity by aldehyde fixation. J. Cell Biol. **17,** 19–58

Saito A., Wang C. T., Fleischer S. (1978): Membrane asymmetry and enhanced ultrastructural detail of sarcoplasmic reticulum revealed with use of tannic acid. J. Cell Biol. **79,** 601–616

Schmalbruch H. (1985): Skeletal Muscle. Springer, Berlin, pp. 82–90

Seagull R. W., Heath I. B. (1979): The effects of tannic acid on the in vivo preservation of microfilaments. Eur. J. Cell Biol. **20,** 184–188

Sjöström M., Squire J. M. (1977): Fine structure of the A-band in cryo-sections. The structure of the A-band of human skeletal muscle fibres from ultra-thin cryo-sections negatively stained. J. Mol. Biol. **109,** 49–68

Slocum R. D., Roux S. J. (1982): An improved method for the subcellular localization of calcium using a modification of the antimonate precipitation technique. J. Histochem. Cytochem. **30,** 617–629

Small J. V. (1981): Organization of actin in the leading edge of cultured cells: influence of osmium tetroxide and dehydration on the ultrastructure of actin meshworks. J. Cell Biol. **91,** 695–705

Smith P. R., Fowler W. E., Pollard T. D., Aebi U. (1983): Structure of the actin molecule determined from electron micrographs of crystalline actin sheets with a tentative alignment of the molecule in the actin filament. J. Mol. Biol. **167,** 641–660

Squire M. J. (1973): General model of myosin filament structure. III. Molecular packing arrangements in myosin filaments. J. Mol. Biol. **77,** 291–323

Suck D., Kabsch W., Mannherz H. G. (1981): Three-dimensional structure of the complex of skeletal muscle actin and bovine pancreatic DNAse I at 6-Å resolution. Proc. Nat. Acad. Sci. USA **78,** 4319–4323

Taylor K. A., Amos K. A. (1983): Structure of actin in reconstructed images of S-1 decorated filaments; a further comment. In: Actin, Structure and Function in Muscle and Non-Muscle Cells (Eds. dos Remedios, C. G., Barden J. A.), pp. 25–26, Academic Press, Sydney

Tilney L. G., Bryan J., Bush D. J., Fujiwara K., Mooseker M. S., Murphy D. B., Snyder D. H. (1973): Microtubules: evidence for 13 protofilaments. J. Cell Biol. **59,** 267–275

Toyoshima C., Wakabayashi T. (1985): Three-dimentional image analysis of the complex of thin filaments and myosin molecules from skeletal muscle. V. Assignment of actin in the actin-tropomyosin-myosin subfragment-1 complex. J. Biochem. **99,** 245–263

Trinick J., Cooper J., Seymour J., Egelman E. H. (1985): Cryo-electron microscopy and three-dimensional reconstruction of actin filaments. J. Microsc. **141,** 349–360

Trinick J., Elliott A. (1982): Effect of substrate on freeze-dried and shadowed protein structures. J. Microsc. **126,** 151–156

Unwin P. N. T. (1974): Electron microscopy of the stacked disk aggregate of tobacco mosaic virus protein. II The influence of electron irradiation on the stain distribution. J. Mol. Biol. **87,** 657–670

Varriano-Marston E., Franzini-Armstrong C., Haselgrove J. C. (1987): Structure of the M-band. J. Electron Microsc. Technique **6,** 131–141

Wacker I., Reiss H. D., Schnepf E., Traxel K., Bauer R. (1986): Polar distribution of calcium- and phosphorus-rich globules induced by glutaraldehyde/tannic acid fixation in the caulonema tip cell of the moss, Funaria hygrometrica: light microscopy, transmission electron microscopy (TEM), proton microprobe (PIXE), and electron spectroscopic imaging (ESI). Eur. J. Cell Biol. **40,** 94–99

Wolosewick J. J., Porter K. R. (1979): Microtrabecular lattice of the cytoplasmic ground substance. Artifact or reality. J. Cell Biol. **82,** 114–139

Final version accepted August 29, 1988